scientific reports

Check for updates

OPEN

Study on jet dynamic impact performance under the influence of standoff

Yizhen Wang, Jianping Yin✉, Xuepeng Zhang✉, Jianya Yi & Xudong Li

Due to the sensitivity of the shaped charge jet to standoff and the complexity of its impact under lateral disturbances, this study aims to investigate the dynamic impact evolution of the jet influenced by standoff and lateral disturbances. A finite element model for the dynamic impact of shaped charge jets was established. Dynamic impact experiments were designed and conducted to validate the effectiveness of the numerical simulations. Utilizing dimensional analysis, a predictive model was developed for jet dynamic impact considering the combined effects of target plate strength, standoff and lateral disturbances. The results indicate that as the standoff varies between 90 mm and 225 mm, the dynamic impact depth of the jet decreases approximately linearly with increasing standoff. Meanwhile, for lateral disturbance velocities ranging from 100 m/s to 400 m/s, the impact depth decreases exponentially with increasing lateral relative velocity of the target. The lateral disturbance velocity is identified as the primary factor influencing jet impact, while the standoff is a secondary factor. The agreement among computational results, numerical simulations, and experimental outcomes confirms the accuracy and effectiveness of the predictive model and simulations, providing a basis for evaluating the dynamic impact potential of shaped charges.

Keywords Jet, Standoff, Impact, Lateral disturbance, Dimensional analysis, Dynamic test

Shaped charge jets utilize the Munroe effect to collapse the liner along the axis, generating high-temperature and high-velocity jets that impact the target[1,2]. As a widely applied technology, jets have demonstrated exceptional effectiveness across various scenarios, with a well-established theoretical foundation[3–6]. During the impact process, the jet elongates while creating a cavity. However, the targets are often not stationary and may possess a relative velocity, particularly when they exhibit significant lateral motion. This lateral movement can induce bending, deviation, or even fragmentation of the jet during impact, which markedly differs from common static impact processes and negatively impacts impact capability. Thus, a comprehensive analysis of the dynamic impact process of jets is essential for accurately estimating their damage performance under dynamic conditions.

For the dynamic impact process under transverse disturbance, domestic and foreign scholars have also carried out some preliminary research[7,8]. Frankel et al.[9] analyzed the influence of target lateral motion on projectile impact performance by using fluid dynamics model, and studied the change of impact velocity and streamline shape with the corresponding ratio of target to projectile velocity and density. Luttwak et al.[10] established a yaw model and studied the erosion of the long rod during the perforation of the moving plate and the possible bending or deflection of the residual rod by numerical simulation. Helte[11] analyzed the cause of the disturbance caused by the interaction between the jet and the flying plate of the reactive armor; Yadav[12] studied the interaction between shaped charge jet and moving target on the basis of simplifying the assumption of constant velocity of jet and target. Zhu et al.[13] analyzed the change of explosive armor interference during jet impact by experiments. Li et al.[14] designed a compressible model of shaped charge jet penetrating radial reaming; Jia et al.[15] analyzed the interaction mechanism between shaped charge jets and thick moving targets, carried out detailed theoretical analysis for each stage and established theory algorithms of changes of cavity when shaped charge jets penetrate the thick moving target. impact depth of undistributed jet, the lateral velocity of jet and impact depth contributed by distributed jet; Han[16] numerically simulated the impact of jets on moving target plates at various incidence angles, revealing fundamental principles of jet impact during oblique impacts.

Reviewing the available literature, most researchers have concentrated on static impact theories or disturbances in thin targets like flyer plates[17–20]. There is a lack of research on the dynamic impact behavior of energetic jets against thicker targets, particularly under lateral perturbations and models to predict their dynamic impact power. In particular, there are few dynamic impact tests for shaped charge jets under high-

School of Mechanical and Electrical Engineering, North University of China, Taiyuan 030051, Shanxi, China. ✉email: yjp123@nuc.edu.cn; zhangxp@nuc.edu.cn

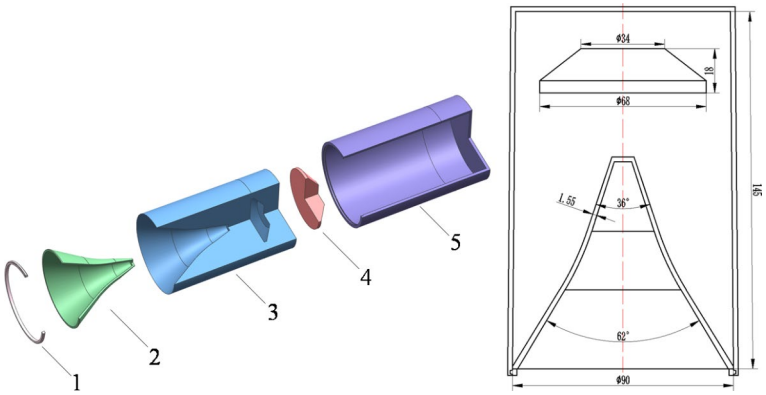

Fig. 1. Simplified physical model and charge structure. (1) Ring (2) Liner (3) Charge (4) Wave Shaper (5) Shell.

Material	ρ/kg·m^{-3}	A/GPa	B/GPa	C	*N*	M
Copper	8960	0.09	0.290	0.025	0.31	1.09

Table 1. Material parameters of liner.

speed lateral disturbances and related engineering models for rapid prediction of jet dynamic impact power.To address this issue, this study proposes a testing method utilizing a rocket sled as the propulsion device to conduct dynamic impact experiments of jets under high-speed lateral disturbances. The experimental data will validate the effectiveness of numerical simulations. Subsequently, based on dimensional analysis, an engineering model will be developed to account for the combined effects of standoff, target plate strength, and lateral disturbances on dynamic impact depth. Finally, cross-comparison analysis between experimental results and numerical simulations will be conducted to verify the applicability of the engineering model.

Model and research plan

Simplified model and numerical simulation

The numerical simulation modeling involved in this study uses TrueGrid software for three-dimensional modeling and numerical simulation of a half model. The symmetry plane is set at the symmetry plane. For the air domain, a non-reflective boundary is set to make the eular material flow freely. To simulate the reality while reducing the length of numerical simulation, the LS-DYNA single-precision version solver provided by the school was used to simulate the dynamic impact process of the shaped charge under lateral disturbance. The target plate employs a Lagrangian algorithm, while other components utilize an Eulerian algorithm. The model integrates a fluid-structure interaction (FSI) approach to simulate the formation of the jet and its impact into the target plate, effectively capturing the significant deformation caused by target interactions during impact. The model's mesh consists entirely of hexahedral elements.

As shown in Fig. 1, the configuration of the shaped charge includes a casing, pressure ring, explosive, waveform shaper, and liner. The detonation is initiated from the center at the bottom. A simplified model of the shaped charge is depicted in Fig. 1. The casing is made of 2024-T3 aluminum alloy, the liner is copper, the explosive used is 8701, and the waveform shaper is composed of phenolic resin. The liner has a diameter of 90 mm and a length of 145 mm, featuring a constant wall thickness conical-arc-conical design with a wall thickness of 1.55 mm. The upper and lower cone angles of the liner are 62° and 36°, respectively. To account for the symmetry in the dynamic impact process of the jet, the numerical simulation employs a half-model at a 1:1 scale.

Material and parameters

The liner utilizes the Johnson-Cook material model along with the Gruneisen state equation[19] to describe the strength properties of materials capable of withstanding large strains and high strain rates. The parameters are detailed in Table 1.

In this context, *A* represents the initial yield stress of the material at the reference strain rate and temperature, while *B* and *N* denote the strain hardening modulus and hardening exponent at the same reference conditions. *C* is the strain rate enhancement parameter, and *M* is the thermal softening parameter.

The explosive used is comp B, modeled using the HIGH_EXPLOSIVE_BURN material model with a JWL equation of state[20]. The material parameters and state equation expressions are sourced from the literature[21].

$$P = A\left(1 - \frac{\omega}{R_1 V}\right)e^{-R_1 V} + B\left(1 - \frac{\omega}{R_2 V}\right)e^{-R_2 V} + \frac{\omega E_0}{V'} \tag{1}$$

Parameters	Values	Parameters	Values
δ/(kg·m^{-3})	1717	R_1	4.2
D/(m·s^{-1})	8320	R_2	1.1
PCJ	0.37	E_0	0.102
A/GPa	524.23	ω	0.34
B/GPa	7.68		

Table 2. Material parameters of explosive.

Materials	C	Si	Mn	Mo	Cr	Re
Ratio(%)	0.26	0.30	1.05	0.60	0.80	0.07

Table 3. Chemical composition of 30CrMnMoRE.

材料	ρ/kg·m^{-3}	E/GPa	v	σ_Y/GPa	β
2024-T3 Aluminum alloy	2780	72.4	0.33	0.345	0.5
Phenol formaldehyde resin	1130	0.35	0.36	0.12	1
30CrMnMoRE	7830	202.8	0.3	0.975	1

Table 4. Material parameters of shell, wave shaper and target plate.

Here, P represents the isentropic pressure, V is the relative volume of the detonation products, and E_0 is the initial internal energy. The parameters are detailed in Table 2.

The shell and the fixed ring are made of 2024-T3 aluminum alloy, which is used to securely fasten the explosive and the liner together. The target plate material is 30CrMnMoRE, with its material properties detailed in Table 3.

The wave shaper is made of phenolic resin. The shell, fixed ring, waveform shaper, and target plate are all modeled using the PK constitutive model[22]. The material parameters for the shell, waveform shaper, and target plate are listed in Table 4.

Here, E represents Young's modulus, v denotes Poisson's ratio, and σ_Y is the yield stress of the material.

Research on grid sensitivity

In order to analyze the influence of grid size on numerical simulation, we selected numerical simulation models with grid side lengths of 0.8 mm, 1.0 mm, 1.5 mm and 2.0 mm respectively to carry out numerical simulation under the same working conditions as the research content of this paper. The numerical simulation results are compared with the experimental data, and the results are shown in Fig. 2.

It can be seen from Fig. 2 that the head velocity of the jet hitting the target obtained in the experiment is 10531.14 m/s. For different mesh sizes, the relative errors compared with the experiment are 0.41%, 3.82%, 6.08% and 13.15% respectively. Obviously, when the mesh size is greater than 1.0 mm, the relative error between the numerical simulation and the test begins to diverge, and the numerical simulation cannot describe the actual situation well. At the same time, the operation time of numerical simulation is analyzed under each grid size. It is found that the time required for numerical simulation increases exponentially with the decrease of grid size. When the grid size is 0.8 mm, the operation time is increased by about 5.99 times compared with the 1.0 mm grid, while the relative error is only increased by 3.41%, which is not significant. In this regard, the numerical simulation used in this paper adopts a grid with a side length of 1.0 mm.

Validation of numerical simulation accuracy

Dynamic impact test

To validate the accuracy of the numerical simulation results, a dynamic testing system for shaped charge jets was employed. The entire dynamic testing system primarily consists of a rocket sled track, a carriage, an impact detonator, a probe, a shaped charge, a rocket engine, protective devices, and the target plate along with testing equipment, as shown in Fig. 3(a).

The shaped charge was fixed vertically to the track toward the target using a bracket on the carriage. The rocket engine was connected to the carriage, with the shaped charge positioned at the front of the carriage, oriented perpendicular to the direction of motion. The rocket engine propelled the warhead forward, and after accelerating to the desired speed, the carriage exited the track. A probe was located at the front of the carriage, equipped with a collision switch at the probe's end. Upon impact with a stop at the track's end, the probe transmitted an electrical signal to the detonator on the warhead, initiating the explosion of the shaped charge and forming a jet directed downward to strike the horizontally positioned target plate. In this dynamic experiment, the arrangement of the rocket sled is shown in Fig. 3(b).

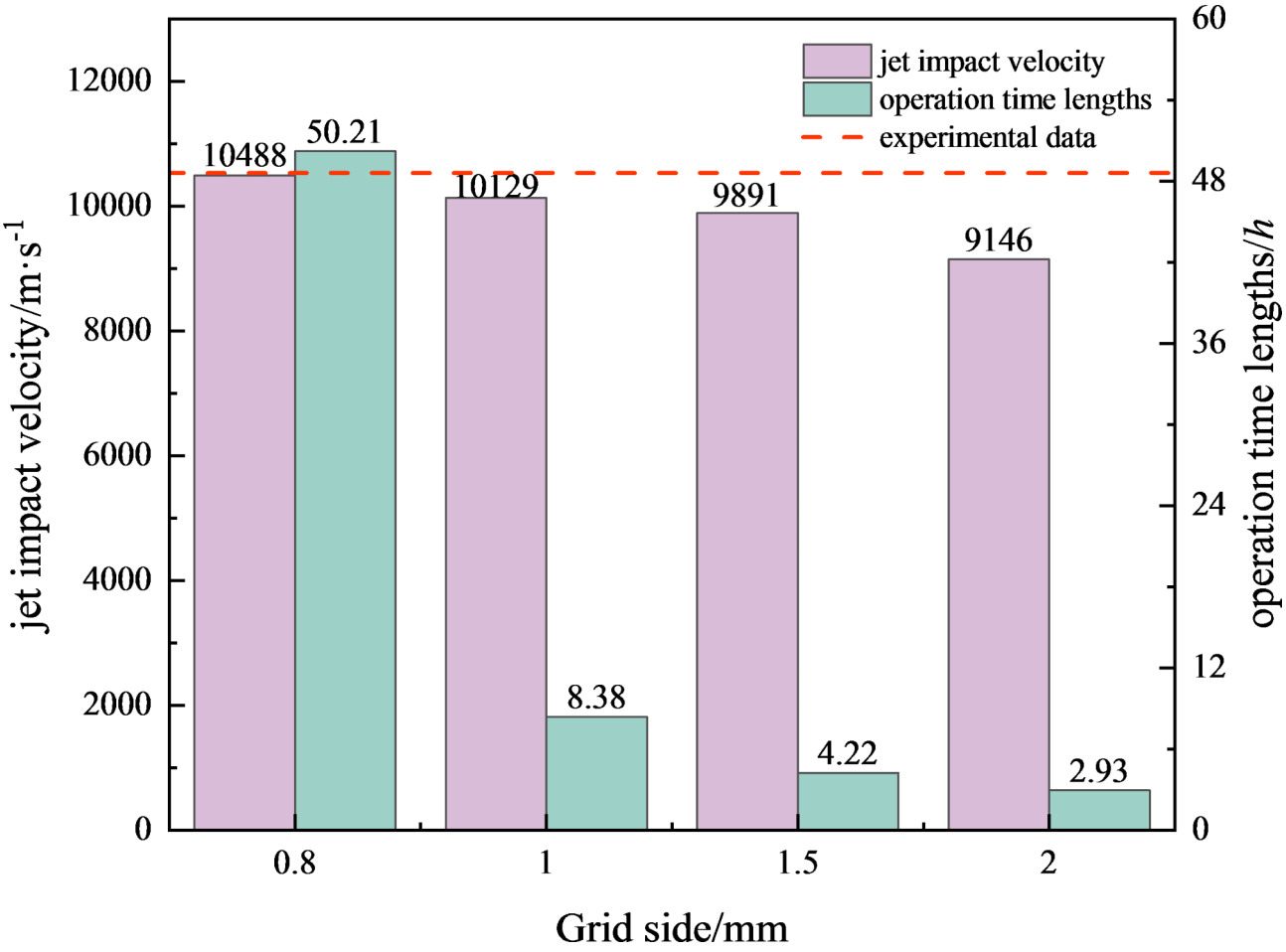

Fig. 2. Sensitivity analysis of mesh size.

During the experiment, to obtain jet velocity data at different target plate thicknesses, measurement devices were installed on the target's surface and at distances of 120 mm and 180 mm behind the target, as illustrated in Fig. 3(c).

The velocity measurement device consists of two layers of electrical signal triggering units and a fixed-height plate. The two layers of aluminum foil are separated by an insulating layer and then encapsulated as a single unit. Wires are attached to each layer of aluminum foil; when the jet has not yet passed through the triggering unit, the circuit remains open. Once the jet passes through, it damages the insulating layer between the aluminum foils, allowing them to conduct and forming a circuit, which outputs an electrical signal.

The plate used to control the standoff establishes the distance between the two triggering units, and by recording the time difference of the electrical signals triggered by both layers, the velocity of the jet at that location can be determined. The structure schematic of the speed measurement device is shown in Fig. 4(a). The target arrangement in the dynamic test is depicted in Fig. 4(b).

As shown in Fig. 4(b), the standoff h is the difference between the charge altitude h_j and target altitude h_b. In the experiment, the base and track of the rocket sled are fixed on the ground. In order to maintain the stability of the rocket sled during the movement, the shaped charge is also fixed on the rocket sled without adjustment, that is, the height h_j of the shaped charge from the ground is fixed; in order to obtain different standoff h for the test, we stack different numbers of target plates at the bottom layer when the target is arranged, so as to change the h_b from the ground, and then adjust the standoff h.

The shaped charge structure used in the experiment primarily includes ring, liner, the main explosive, wave shaper, auxiliary charge, casing, and detonator. Its structural schematic is shown in Fig. 5.

High-speed photographic recordings of typical jet dynamic impact tests are shown in Fig. 6.

Reliability verification of numerical simulations

To simulate the propagation of explosives in real-world scenarios, a numerical model was established based on the jet formation process and the compression mechanism of the detonation wave on the liner. An air domain was maintained around the shaped charge to allow the explosive to flow freely, while non-reflective boundaries were set on the outer surface of the air domain to reduce computational time while ensuring accuracy. The mesh size for the air domain was set to 1 mm × 1 mm × 1.5 mm. The target plate structure was modeled according to

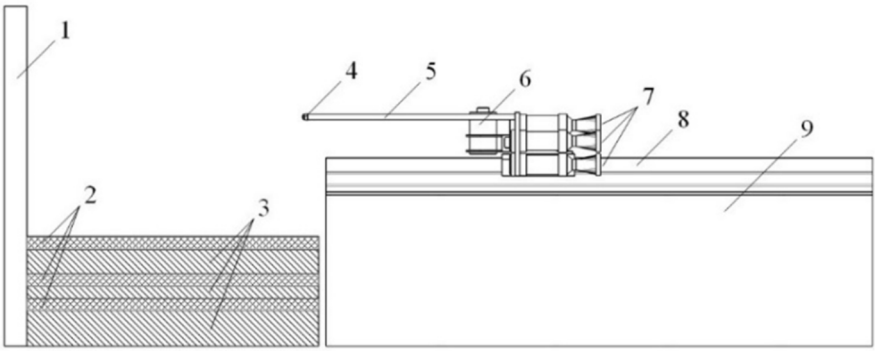

1. Barrier 2. Velocity Measurement Device 3. Target Plate 4. Piezoelectric Fuze

5. Probe 6. Shaped Charge 7. Rocket Engine 8. Rail 9. Rail Base

(a) Schematic of Dynamic Test System

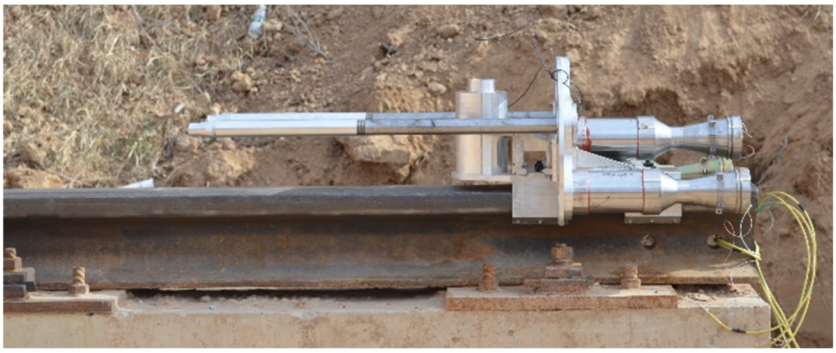

(b) Arrangement of the rocket sled in the experiment

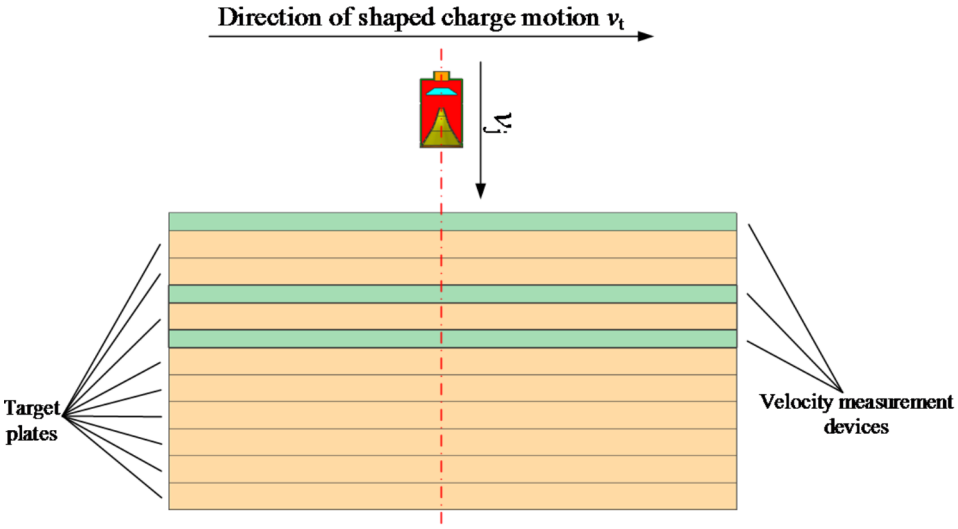

(c) Schematic of Dynamic Test Principle

Fig. 3. Schematic of Dynamic Test.

the actual experimental setup. The three measurement devices, made of lightweight materials like honeycomb paper, plastic film, and aluminum foil, had minimal impact on the jet impact process and were therefore omitted in the numerical simulation. The numerical simulation model is shown in Fig. 7.

Numerical simulations based on experimental conditions revealed that lateral movement of the target plate significantly negatively impacted jet impact. During the impact process, the channel walls struck the jet, causing instability, deflection, or even fracture, which greatly diminished its impact capability. This interference prevented subsequent jets from advancing through the channels created by earlier jets, reducing their contribution to

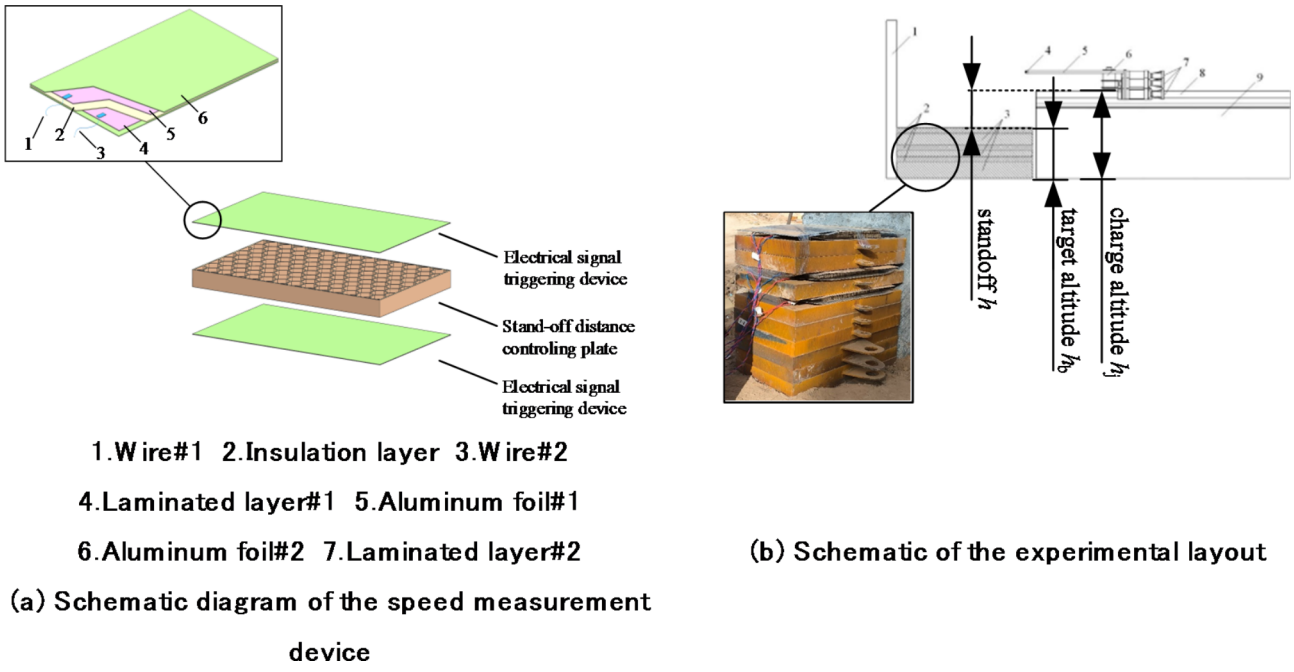

Fig. 4. Arrangement of equipment in dynamic experiments.

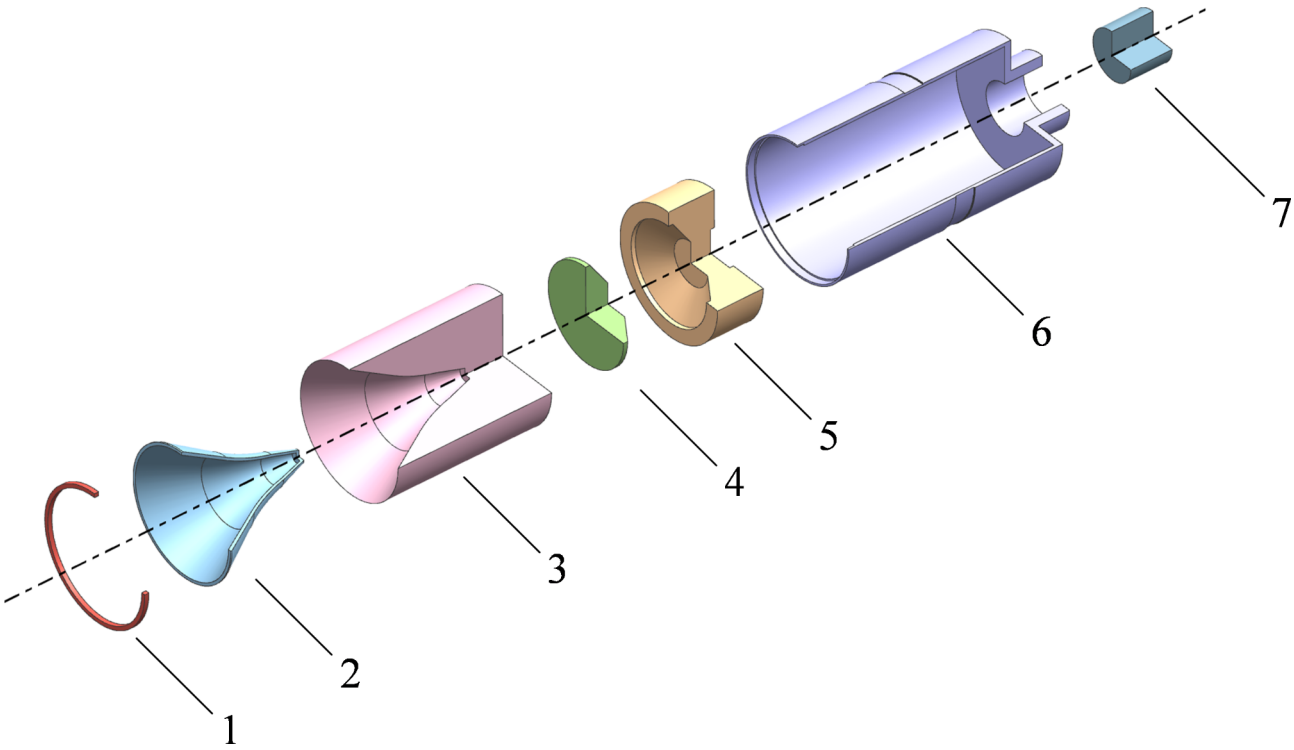

Fig. 5. Schematic of shaped charge structure. 1.ring 2.liner 3.main explosive 4.wave shaper 5.auxiliary charges 6.casing 7.detonator.

overall impact depth. The jet penetrated two layers, totaling 120 mm, and partially affected the third layer but did not penetrate it, ultimately accumulating at the bottom of the jet channel. The dynamic impact process of the jet in the numerical simulation is illustrated in Fig. 8(a).

Analysis of the jet's effects on each layer of the target plate was conducted, selecting three representative scenarios, as shown in Fig. 8(b). The jet caused substantial damage at the impact surface of the first layer,

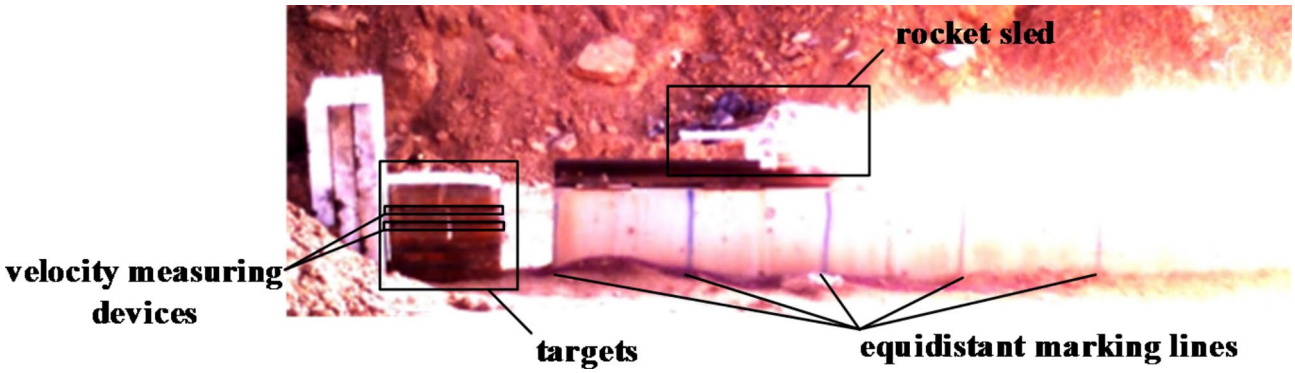

Fig. 6. Photograph of jet dynamic impact test.

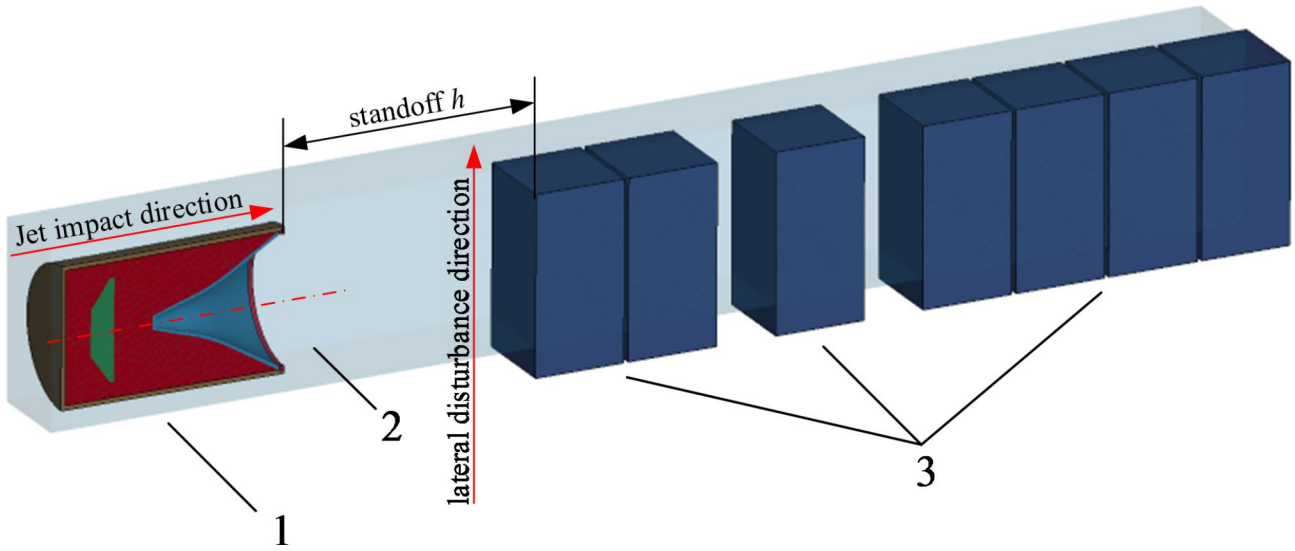

Fig. 7. Numerical simulation model. (1) Shaped charge (2) Air domain (3) Targets.

with noticeable cutting marks due to lateral movement. However, the effect of the target plate on the lateral disturbance of the jet was less pronounced on the back of the second layer and the impact surface of the third layer. This is primarily because the effective penetrating jet concentrated at the head, which possessed higher kinetic energy, allowing it to overcome lateral disturbances to some extent.

In the numerical simulation, the impact failure form, failure effect and perforation diameter of the incident surface and the back of each layer of the target plate are similar. Combined with the numerical simulation and experimental results, the jet causes a large damage on the incident surface of the first layer of the target plate, and there are obvious cutting marks on it due to the lateral movement. Combined with the existing impact and reaming theory, it can be seen that the cutting effect on the first layer of the target plate is caused by the transverse relative motion between the micro-element in the middle and rear section of the jet and the target plate. In this part, the velocity of the jet micro-element is relatively low, and the reaming ability is also weak. Therefore, it will be pushed by the transverse disturbance and collide with the channel wall, and finally leave the cutting trace in the area near the surface of the target plate.

On the back of the second layer and the front of the third layer, the lateral disturbance effect of the target plate on the jet is not obvious. This is mainly because the jet capable of further effective impact of the target plate is mainly concentrated in the jet head, which carries a higher kinetic energy and has a greater ability to expand the hole on the target plate, so that it can overcome the lateral disturbance to a certain extent. Impact, it is worth noting that this part of the jet element in the process of reaming and impact, is also constantly losing energy, and due to the influence of lateral disturbance, the impact process by one side of the numerical simulation can better reproduce the test results.

In addition, combined with Fig. 8 (c), it can be seen that the jet has a high velocity when it contacts the target plate, and after penetrating the second layer of the target plate, the velocity of the jet head has a significant attenuation, which is reduced to 4666.67 m/s, a decrease of about 51%. Because the jet does not penetrate the third layer, the speed measuring device between the 3–4 layers does not collect data. Comparing the dynamic test with the numerical simulation results, it can be seen that the relative errors between the numerical simulation

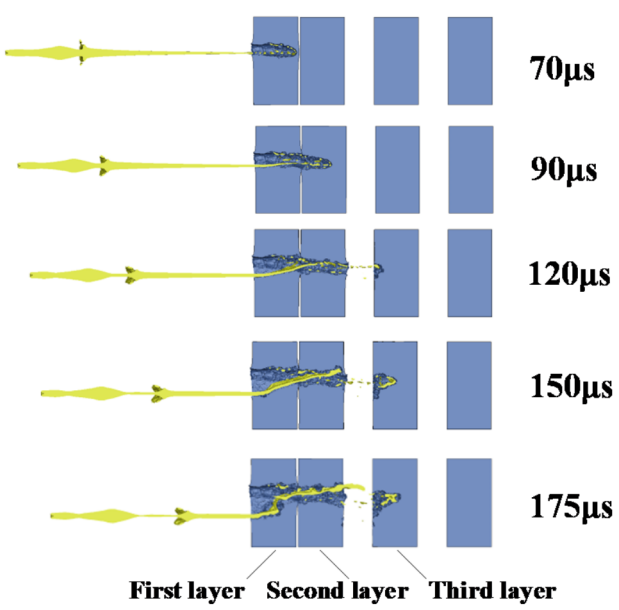

(a) Jet dynamic impact process

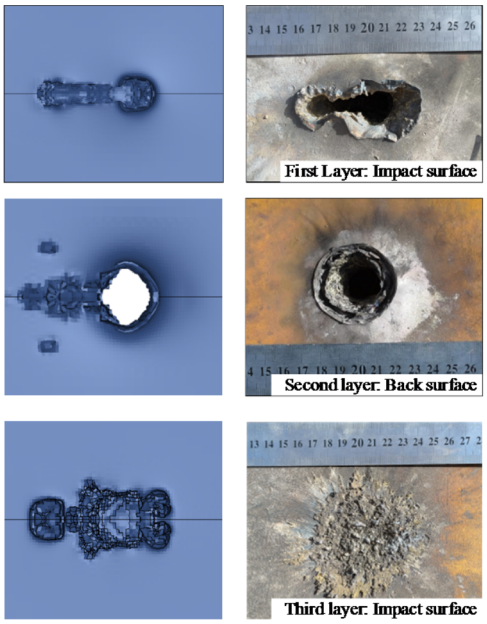

(b) Comparison of numerical simulations and experimental results

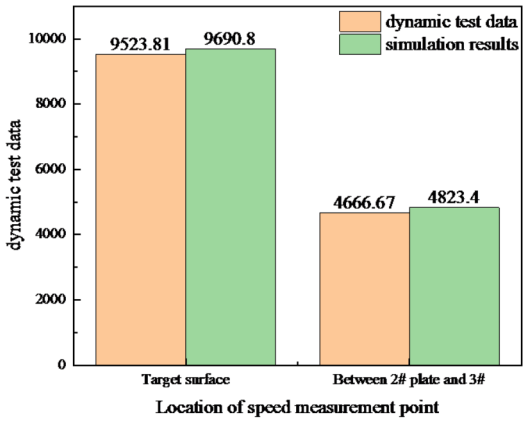

(c) Comparison of jet dynamic penetration velocity measurement

Fig. 8. Analysis of numerical simulation results.

and the test results are 1.75% and 3.36%, respectively, and the jet velocities at different positions have good consistency.

By analyzing the potential error factors in Fig. 8, it is found that this is mainly due to the fact that in the actual test, the shaped charge is driven by the rocket pulley, so as to simulate the influence of lateral disturbance on the jet impact process. In the process of flight, there are many unstable factors, such as the vibration of the parts of the pulley and the shaped charge, the influence of air resistance, the flatness of the track and so on, which all affect the final dynamic impact results of the jet. And for the shaped charge, the impact depth itself also has a certain beating[25].

Therefore, there is a certain range of error between the numerical simulation and the experimental results.

Jet dynamic impact model establishment

Analysis of the impact of standoff and lateral disturbances on jet impact

In order to study the influence of standoff on the dynamic impact of jet, the dynamic impact process of jet is studied when the standoff h changes in the range of 1D(90 mm), 1.5D(135 mm), 2D(180 mm) and 2.5D(225 mm), and the transverse disturbance velocity v_t is 100 m/s, 200 m/s, 300 m/s and 400 m/s. A total of 16 sets of numerical simulations were performed, and the resulting data are plotted as shown in Fig. 9(a).

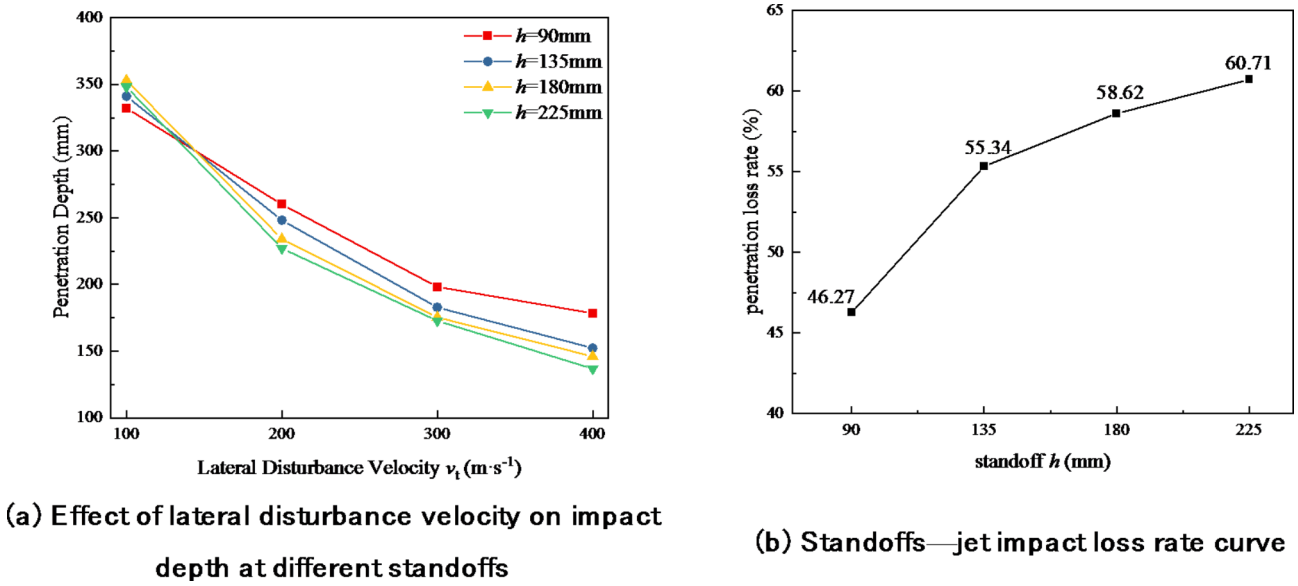

Fig. 9. Impact of lateral disturbance on jet impact at varying standoffs.

From Fig. 9(a), it can be observed that as the lateral disturbance velocity increases, the dynamic impact depth of the jet decreases consistently, regardless of whether the detonation height varies between 90 mm and 225 mm. For different detonation heights, the jet exhibits an approximately exponential decay trend with increasing lateral disturbance velocity, initially decreasing rapidly and then gradually slowing the rate of decline.

Extensive theoretical, numerical, and experimental studies indicate that during the formation and impact of shaped charges, the presence of a velocity gradient causes the jet to elongate. Considering the conservation of energy and mass, the jet diameter must continuously decrease, becoming increasingly slender until it breaks into smaller segments. During the static impact process, the reduction in jet diameter during stretching has a negligible effect on overall impact power. Most studies suggest that maintaining the continuity of the jet during impact enhances its performance.

However, for the dynamic penetration process of the shaped charge jet, the jet is inevitably affected by the channel wall due to the existence of the lateral motion of the target during the penetration process, and the penetration ability of the jet in contact with the channel wall is greatly reduced. In this regard, it is necessary to consider the resistance of the jet under lateral disturbance. In order to characterize the fluctuation of the dynamic penetration depth of the jet under the influence of different standoff distances and lateral disturbance velocities, we define the penetration loss rate χ_h as the reduction of the dynamic penetration depth P of the jet when the lateral disturbance velocity v_t increases from 100 m/s to 400 m/s under the same standoff distance h. It can be expressed by Eq. (1) :

$$\chi_h = \frac{P_{h,v_t=100} - P_{h,v_t=400}}{P_{h,v_t=100}} \times 100\% \tag{1}$$

Based on Eq. (1), the attenuation rate of jet penetration depth is drawn as shown in Fig. 10(b). When increasing from 100 m/s to 400 m/s, the loss rate of jet penetration depth increases from 46.27 to 60.71%. Compared with other larger explosion heights, the attenuation of jet dynamic penetration depth at 90 mm explosion height is smaller. That is, the diameter of the jet formed at a smaller standoff distance is larger, and its penetration performance under lateral disturbance is better than that of the large standoff distance.

The 16 sets of numerical simulation results are compared, as shown in Fig. 10.

It is found from Fig. 10 that when the lateral disturbance velocity is less than or equal to 100 m/s, the jet penetration depth increases first and then decreases with the increase of the standoff distance, which indicates that when there is a low-speed lateral disturbance, there is an optimal standoff distance for this type of shaped charge jet, which is near 180 mm. When the lateral disturbance velocity is greater than 100 m/s, the dynamic penetration depth of the jet decreases monotonously with the increase of the standoff distance. It shows that when the jet changes from static penetration to dynamic penetration with lateral disturbance, the optimum burst is about 1 times higher than the current charge diameter. That is, with the increase of lateral disturbance, the optimal standoff distance is getting smaller and smaller. This reflects that in this case, the jet is not fully elongated when contacting the target plate, but has a relatively large diameter, which is helpful for the dynamic penetration of the jet when it is subjected to high-speed lateral disturbance.

Establishment of the predictive model

To conduct a dimensional analysis of the physical quantities affecting the residual velocity of the projectile's impact, we consider the specific conditions of this study. Given that the explosive composition remains the same

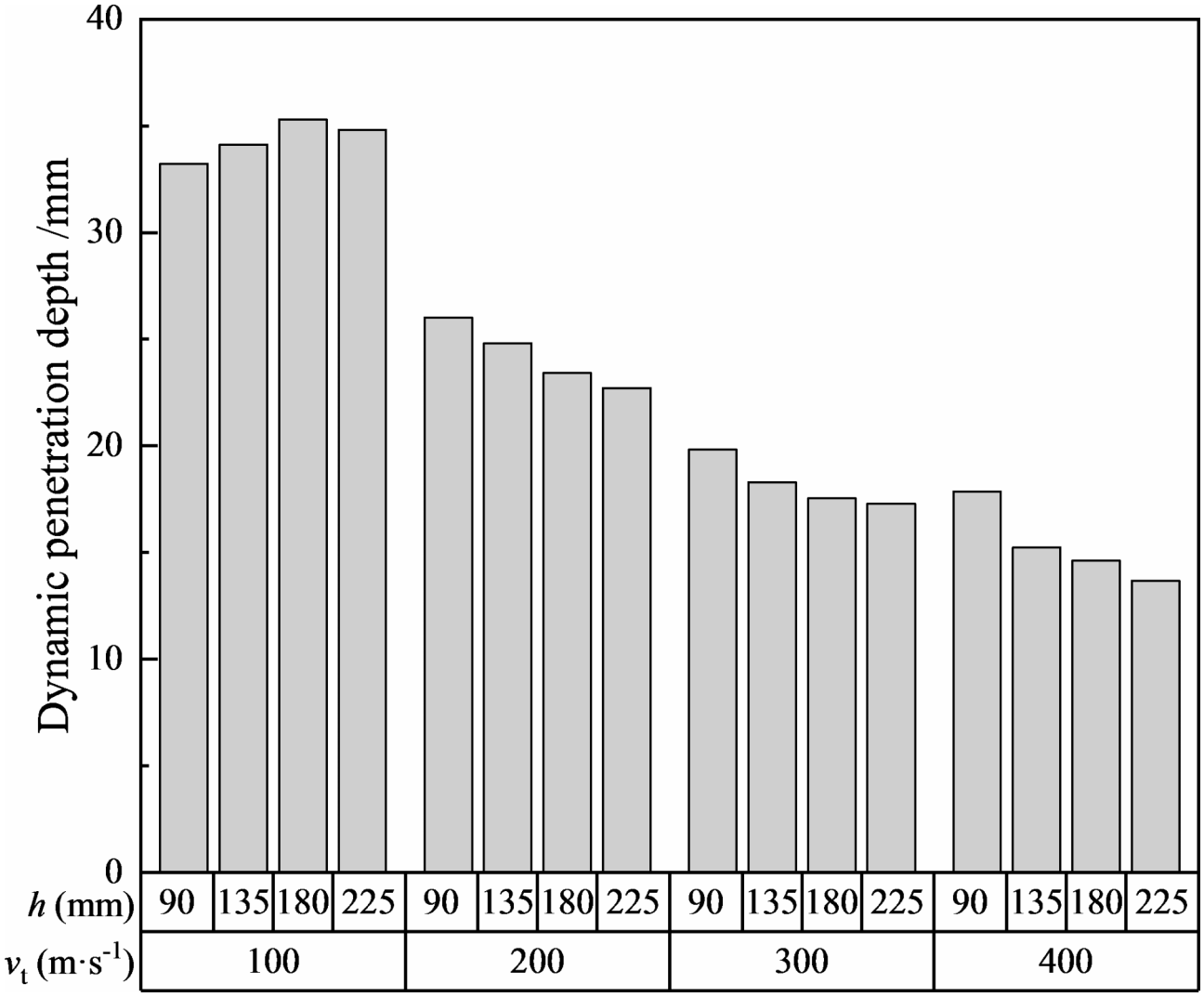

Fig. 10. Dynamic impact depth of jet under different standoff and lateral disturbance velocities.

under different conditions, factors such as explosive density, detonation velocity, and energy density of charge can be disregarded. However, since the jet dynamic impact process is complex, the densities and strengths of the jet and target materials play a crucial role and cannot be ignored.

The selected parameters for this analysis include:

- Height of the liner H.
- Diameter of the liner D.
- Liner thickness T.
- Cone angle of liner α.
- Length of charge A.
- Standoff h.
- liner density ρ_j
- Target plate density ρ_t
- Elastic modulus of the target E_{ty}
- Yield strength of the jet Y_j
- Yield strength of the target Y_t
- Hardening modulus of the target E_{tt}
- Ultimate strength of the target Y_{ts}
- Failure strain of the target ε_{tf}
- Lateral velocity of the target v_t

Additionally, μ_j and μ_t represent the Poisson's ratios of the warhead casing and the target materials, respectively.

The expression for the dynamic impact depth P_{jv} of the jet can be formulated as a function of these parameters. A general form might be:

$$P_{jv} = f(H, D, T, \alpha, A, h, \rho_j, \rho_t, E_{ty}, Y_j, Y_t, E_{tt}, Y_{ts}, \varepsilon_{tf}, v_t, \mu_j, \mu_t) \tag{2}$$

Where f is a function that encapsulates the relationships among these parameters based on dimensional analysis and empirical correlations. Further derivation would require experimental data to establish the specific form of f.

Given that the elastic modulus, density, and Poisson's ratio of the two target materials are very similar, the influences of ρ_t, E_{ty}, and μ_t can be neglected. Furthermore, for the warhead casing made of the same material, the Poisson's ratio μ_j remains consistent.

Thus, the expression for the dynamic impact depth P_{jv} can be simplified, omitting those parameters. The revised expression could be represented as:

$$P_{jv} = f(\rho_j, h, Y_j, H, D, T, A, v_t, Y_t, E_{tt}, Y_{ts}, \alpha, \varepsilon_{tf}, \mu_t) \tag{3}$$

This reflects the primary influencing factors, focusing on the parameters that significantly affect the impact dynamics. Further empirical analysis would be required to fine-tune this expression.

This reflects the primary influencing factors, focusing on the parameters that significantly affect the impact dynamics. Further empirical analysis would be required to fine-tune this expression.

To establish a dimensional analysis using the selected reference physical quantities—jet density ρ_j, nozzle diameter D, and jet yield strength Y_j—we can define the dimensional indices for each parameter.

The dimensional index matrix A can be represented as follows:

$$|A| = \begin{vmatrix} 1 & 0 & 1 \\ -3 & 1 & -1 \\ 0 & 0 & -2 \end{vmatrix} = 1 \neq 0 \tag{4}$$

Since the determinant is non-zero and the three reference quantities are dimensionally independent, any one of these quantities cannot be expressed in terms of the other two. Thus, they form a set of fundamental quantities.

For the dimensional analysis of the selected reference quantities, we can express the dimensionless relationship in the following form:

$$\frac{P_{jv}}{D} = f(, \frac{H}{D}, \frac{h}{D}, \frac{T}{D}, \frac{A}{D}, v_t\sqrt{\frac{\rho_j}{Y_j}}, \frac{Y_t}{Y_j}, \frac{E_{tt}}{Y_j}, \frac{Y_{ts}}{Y_j}, \alpha, \varepsilon_{tf}, \mu_t) \tag{5}$$

In the PK model, the Cowper-Symonds model is highly effective. The relationship between dynamic yield stress and strain rate is given by:

$$\sigma_y = \left[1 + \left(\frac{\dot{\varepsilon}}{C}\right)^{\frac{1}{p}}\right](Y_t + \beta E_p \varepsilon_e^p) \tag{6}$$

In the equation, σ_y represents the dynamic yield strength; $\dot{\varepsilon}$ denotes the strain rate; β is the hardening parameter; E_p is the plastic hardening modulus, determined by the elastic modulus E_{ty} and the hardening modulus E_{tt}; and ε_e^p is the effective plastic strain.

Observing Eq. (6), we find that the peak dynamic yield strength, considering strain rate effects, is related to the yield strength, hardening modulus, and failure strain. Specifically, this relationship can be expressed as:

$$\sigma_y \propto Y_t + \beta E_p \varepsilon_{tf} \tag{7}$$

The elastic moduli and densities of the two target plates are very similar, allowing us to disregard the effects of ρ_t and E_{ty}. For the same type of material used in the warhead casing, the jet density ρ_j and the Poisson's ratio μ_j are consistent.

Thus, the terms in Eq. (5) can be appropriately simplified as follows:

$$\frac{P_{jv}}{D} = f(\frac{h}{D}, v_t\sqrt{\frac{\rho_j}{Y_j}}, \frac{\sigma_y}{Y_j}, \varepsilon_{tf}) \tag{8}$$

For the same type of warhead casing, its density ρ_j and yield strength $Y_j$are known quantities. Applying the Π theorem, we can transform Eq. (8) into the following form:

$$\frac{P_{jv}}{D} = R\left(v_t\sqrt{\frac{\rho_j}{Y_j}}\right)^a \left(\frac{\sigma_y}{Y_j}\right)^b \left(\frac{h}{D}\right)^c {\varepsilon_{tf}}^d \tag{9}$$

Here, a, b, c, and d are the coefficients to be determined. Once the values of these four coefficients are established, we can obtain the impact depth under the combined effects of explosive loading and lateral velocity.

From the formula (9), it can be seen that through the given shaped charge and target plate material, the diameter of the liner D, the jet density ρ_j, the jet strength Y_j, the target plate failure strain ε_{tf} and the target plate strength σ_y can be determined; after that, by determining the intersection condition of the projectile and the target, that is, giving the lateral disturbance velocity v_t and the standoff h of the shaped charge, the dynamic impact depth P_{jv} of the jet in this case can be obtained according to the model.

Since the main purpose of this paper is to study the change law of the impact ability of the jet under the transverse disturbance, the formula (9) is simplified accordingly. Assuming that the structure of the shaped charge and the material of the target plate remain unchanged, only considering the influence of the standoff and the transverse disturbance velocity, the formula (9) can be simplified as follows :

$$P_{jv} = \psi {v_t}^b h^c \tag{10}$$

In order to determine the value of the undetermined coefficient in the above expression, the simulation data results are statistically analyzed. The results of the fitted functional relationship are as follows :

$$P_{jv} = 2.958 {v_t}^{-0.643} h^{-0.167} \tag{11}$$

From the formula (11), it can be seen that with the increase of the lateral disturbance velocity v_t, the dynamic impact depth of the jet shows a similar exponential downward trend; for the change of explosion height h, the influence law is similar to that of v_t, but its influence on the dynamic impact of jet is less than that of v_t.

Based on the formula (11), the prediction model of penetration depth under the influence of explosion height and lateral disturbance velocity is drawn as Fig. 11. It can be seen that it is in good agreement with numerical simulation.

The fitting R^2 value of the model to the numerical simulation results is 0.967, that is, the interpretation strength is 96.7%. The prediction model obtained by dimensional analysis is in good agreement with the numerical simulation results, and the consistency with the numerical simulation results is high. According to the prediction model, it can be seen that when the standoff distance changes within 90 mm ~ 225 mm, the increase of the standoff distance is not conducive to the dynamic penetration of the jet, and with the increase of the lateral disturbance velocity, the influence of the change of the standoff distance on the penetration depth of the

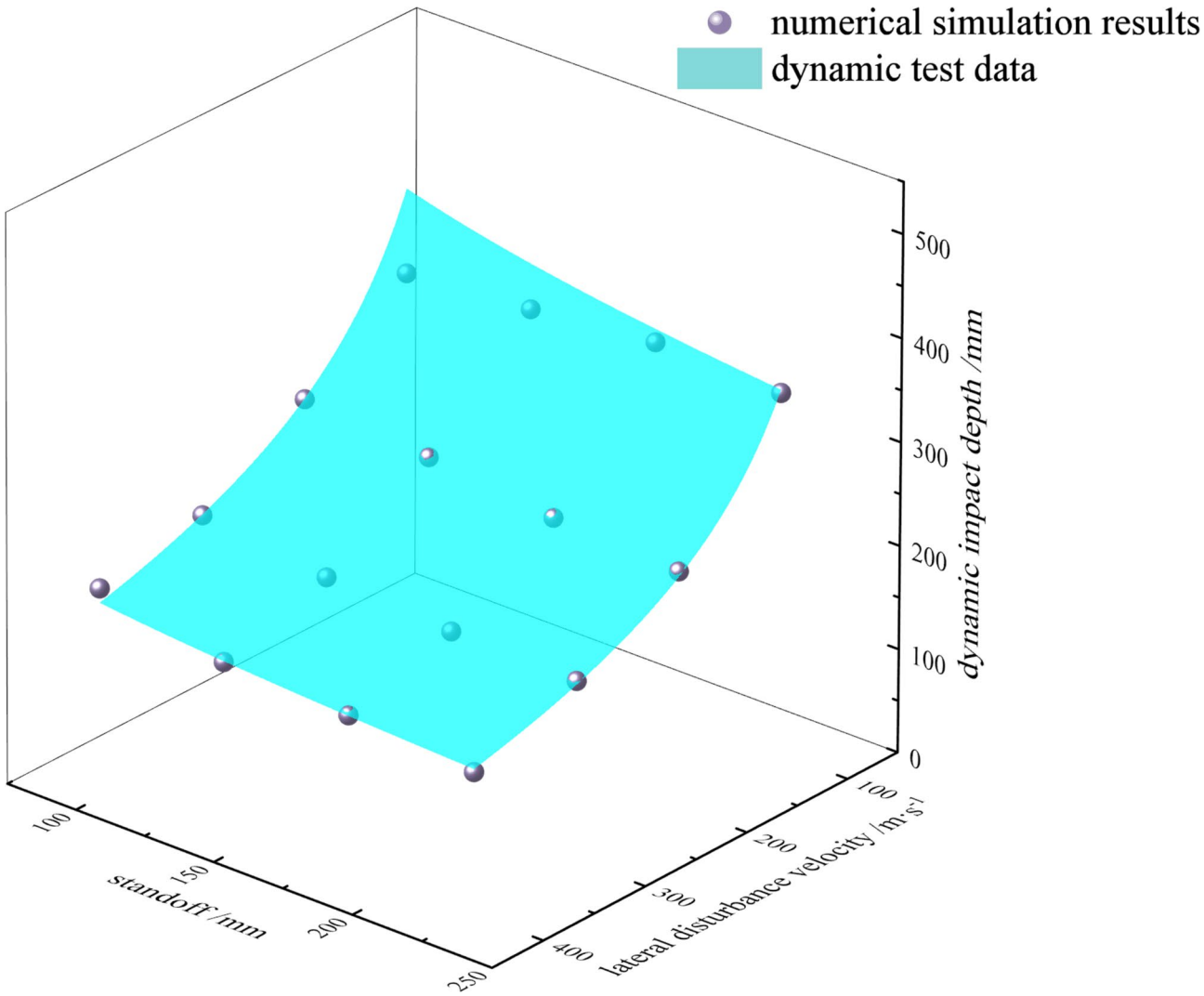

Fig. 11. Prediction model for dynamic impact depth of jets.

jet decreases continuously, that is, in the dynamic penetration process of the jet under the joint influence of the standoff distance and the lateral velocity, the lateral velocity is the main factor affecting the penetration depth of the jet, which is dominant. With the increase of the lateral disturbance velocity, the jet penetration depth shows a nearly exponential downward trend, that is, with the increase of the lateral disturbance velocity, the attenuation rate of the dynamic penetration depth of the jet gradually decreases.

Validation analysis of the predictive model

In order to further analyze the accuracy of the prediction model, three and six rocket engines were used in the dynamic impact test of the jet, and the dynamic impact data of the jet were obtained when v_t=123 m/s, 286 m/s, and the explosion heights were 174 mm and 113 mm, respectively. The results of the engineering prediction model and the dynamic test data are drawn as shown in Fig. 12, and the prediction model is analyzed.

The error of the engineering prediction model to the dynamic test results is less than 15%, and the test results are well predicted. This shows that the engineering prediction model for different standoff. The dynamic impact power of jet under different lateral disturbance velocities is well characterized, and the engineering prediction model is accurate and effective.

According to the predictive model, when the detonation height varies between 90 mm and 225 mm, an increase in detonation height negatively affects jet dynamic impact. Furthermore, as lateral disturbance velocity increases, the impact of detonation height on impact depth diminishes. Thus, in the context of combined detonation height and lateral velocity influences, lateral velocity emerges as the primary factor affecting jet impact depth. As lateral disturbance velocity continues to rise, the jet impact depth exhibits a nearly exponential decline, indicating that the rate of decay in dynamic impact depth decreases with increasing lateral disturbance velocity.

Conclusion

We utilized numerical simulation methods to model the dynamic impact process of shaped charges and conducted dynamic tests to validate the effectiveness of the simulations. This analysis examined the combined effects of detonation height and lateral disturbance velocity on jet impact. Based on dimensional analysis, we

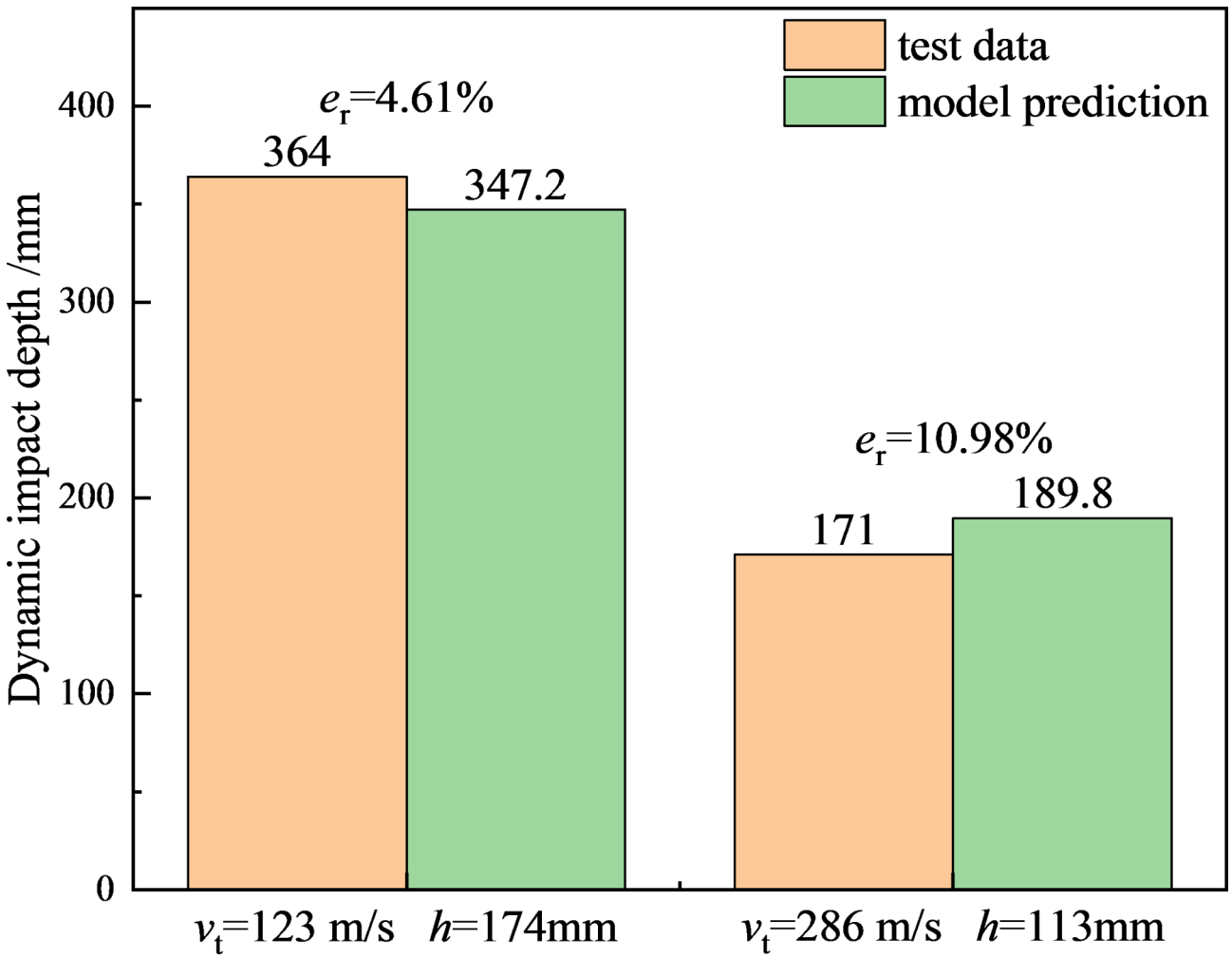

Fig. 12. Prediction model for dynamic impact depth of jets.

established a predictive model for jet dynamic impact depth, validating its applicability through numerical simulations and experimental data. The main conclusions are as follows:

(1) When the lateral disturbance velocity is in the range of 100 m/s ~ 400 m/s and the standoff distance is in the range of 1.0 ~ 2.5D, with the increase of the lateral disturbance velocity, the dynamic penetration depth of the jet increases first and then decreases, and evolves into a monotonically decreasing.
(2) As lateral disturbance velocity increases from 100 m/s to 400 m/s, the impact loss rate of the jet increases with greater standoff; the minimum impact loss rate is 38.92% at a standoff of 90 mm, while the maximum is 50.82% at 225 mm.
(3) Cross-comparison of numerical simulations, experimental data, and the predictive model shows that the relative error of the established model is below 15%, demonstrating good consistency. The engineering model effectively estimates the impact depth of the jet under the combined effects of standoff and lateral disturbance velocity.

Data availability

Data sets generated during the current study are available from the first author(Yizhen Wang) on reasonable request. The experimental data are available from the first author(Yizhen Wang) but restrictions apply to the availability of these data, which were used under license for the current study, and so are not publicly available.

Received: 8 October 2024; Accepted: 12 December 2024
Published online: 28 December 2024

References

1. Xu, W. L., Wang, C. & Xu, B. Investigation of hyper shaped charge jet formation theory. *Acta Armamentarii*. **39** (02), 261–268 (2018).
2. Liu, Y. et al. Deformation and fracture mechanisms and characteristics of long tungsten alloy rod under the lmpact of linear shaped jet. *Acta Armamentarii*. **41** (S2), 135–143 (2020).
3. Zhao Xin, Xu, Y. J. et al. Simulation and optimization research of impact performance of liner . *J. Ordnance Equip. Eng.* **42** (10), 65–71 (2021).
4. Wang, C., Yun, S. R. & Huang, F. L. An experimental study and numerical simulation on annular jet formation and impact . *Acta Armamentarii*. **24** (4), 451–454 (2003).
5. Yin, J. P. *Multiple exsplosively shaped projectile warhead technology[M]* (Bejing National Defense Industry, 2012).
6. Yin, J. P. & Wang, Z. J. *Ammunition [M]* (Bejing National Defense Industry, 2017).
7. Jia, X. et al. Theoretical analysis and experimental study of the performance of shaped charge jet impact into thick-walled moving target by rocket sled testing method. *Int. J. Impact Eng.* **155**, 103894 (2021).
8. Li, J. R. et al. Numerical Study and Theoretical Model of Shaped Charge Jet Penetrating Into Thick-Walled Target With Following Velocity. *Int. J. Aerosp. Eng.*, 7646255. (2024).
9. Frankel, I. & Weihs, D. Hydrodynamic theory of glancing impact. *J. Fluid Mech.* **216**, 213–229 (1990).
10. Luttwak, G. & Luttwak, A. Moving plate perforation analytic model and numerical simulation[C]‖Proceedings of the 21st International Symposium on Ballistics. Adelaide, Australia:International Ballistics Committee, : 976–983. (2004).
11. Helte, A. & Lide, N. E. The role of kelvin-helmholtz instabilities on shaped charge jet interaction with reactive armor plates. *J. Appl. Mech.* **77** (5), 051805 (2010).
12. Yadav, H. S. Interaction of a metallic jet with a moving target . *Propellants Explosives Pyrotechnics*. **13** (3), 74–79 (2010).
13. Zhu, D. B. & Li, J. Y. Disturbance on an armor-piercing jet caused by an explosive armor. *Acta Armamentarii*. **12** (001), 46–53 (1991).
14. Li, G. & Chen, X. W. A compressible model of radial crater growth by shaped-charge jet impact. *Explosion Shock Waves*. **42** (07), 97–105 (2022).
15. Cao, P. et al. Numerical Simulation of Rod Jet Impact Moving Target . *J. Ordnance Equip. Eng.* **42** (04), 86–90 (2021).
16. Han, S. F. *Simulation research on sunder armor oblique penetrate high speed movement[D]* (North University of China, 2015).
17. Tan, L. L., ZhanG, T. & Qiao, L. G. Numerical Simulation of Shaped Jet Penetrating Moving Steel Target. *Ordnance Ind. Autom.* **40** (10), 6–9 (2021).
18. Yi, J. Y. et al. Reaction characteristics of polymer expansive jet impact on explosive reactive armour. *e-Polymers*, **20**(1): 577–601 (2020).
19. Wang, Q., Zhao, H. D. & Zhao, P. D. Study on damage effectiveness of shaped warhead in air defense and anti-missile. *Ordnance Ind. Autom.* **37** (5), 60–63 (2018).
20. Chen, Z. H. *Analysis of the characteristics of the Jet from HEAT projectile with the error and simulation research on impact into the high-speed target in an angle[D]* (North University of China, 2015).
21. Zhao, X. *Study on the Impact Performance of the Warhead of the Electroplated Bimetal Liner [D]* (North University of China, 2015).
22. Li, R. J. et al. Ballistic resistance capabilities of explosive reactive armors encapsulated by ceramic layers. *Explosion Shock Waves*. **34** (01), 47–51 (2014).
23. Wu, J., Liu, J. B. & Du, Y. X. Experimental and numerical study on the flight and impact properties of explosively-shaped projectile. *Int. J. Impact Eng.* **34** (7), 1147–1162 (2007).
24. Jia, X. et al. Theoretical model and numerical study of shaped charge jet penetrating into thick moving target . *Acta Armamentarii*. **40** (08), 1553–1561 (2019).
25. Zhang, F. et al. Effect of materials of auxiliary liner on the formation of high-speed jet by truncated liner. *Acta Armamentarii*. **39** (S1), 52–56 (2018).

Acknowledgements

This work was supported by the Shanxi province basic research program free exploration youth fund project (Grant Nos. 202203021212136).

Author contributions

Y.Z. W. was responsible for conceptualization, methodology, software, validation, investigation, data curation, formal analysis, writing—original draft preparation and project administration. J.P. Y. was responsible for conceptualization, formal analysis, investigation, data curation, writing—review and editing, supervision. X.P. Z.

was responsible for formal analysis, investigation and supervision. J.Y. Y. was responsible for formal analysis, investigation and supervision. X.D. L. was responsible for formal analysis, investigation and supervision. All authors have reviewed and agreed to the published version of the manuscript.

Declarations

Competing interests

We declare that we have no financial and personal relationships with other people or organizations that can inappropriately influence our work, there is no professional or other personal interest of any nature or kind in any product, service and/or company that could be construed as influencing the position presented in, or the review of, the manuscript entitled, "Study on Jet Dynamic Impact Performance under the Influence of Standoff and Lateral Disturbance".

Additional information

Correspondence and requests for materials should be addressed to J.Y. or X.Z.

Reprints and permissions information is available at www.nature.com/reprints.

Publisher's note Springer Nature remains neutral with regard to jurisdictional claims in published maps and institutional affiliations.